buildings

MDPI

Article

Enhancing the Mechanical Properties of Ultra-High-Performance Concrete (UHPC) Through Silica Sand Replacement with Steel Slag

Hadi Bahmani [1], Hasan Mostafaei [1,2,*], Paulo Santos [3,*] and Niyousha Fallah Chamasemani [4]

[1] Department of Civil Engineering, Isfahan University of Technology (IUT), Isfahan 84156-83111, Iran; h.bahmani@cv.iut.ac.ir
[2] School of Civil and Environmental Engineering, University of Technology Sydney, Sydney, NSW 2007, Australia
[3] University of Coimbra, Department of Civil Engineering, ISISE, ARISE, 3030-788 Coimbra, Portugal
[4] Department of Civil and Environmental Engineering, Politecnico di Milano, P.za L. da Vinci 32, 20133 Milan, Italy; niyousha.fallah@mail.polimi.it
* Correspondence: hasan.mostafaei@student.uts.edu.au (H.M.); pfsantos@dec.uc.pt (P.S.)

Abstract: In modern construction, increasing the sustainability of materials without sacrificing performance is crucial. Ultra-High-Performance Concrete (UHPC) is known for its exceptional strength and durability. However, incorporating waste and optimizing the mix is still a key focus. The main goal of this article is to evaluate the enhancement of the mechanical properties of UHPC by replacing silica sand with steel slag at various percentages (25%, 50%, 75%, and 100%). With this purpose, we measured the compressive, tensile, and flexural strengths, as well as relative density and water absorption. It was found that the best mechanical performance of UHPC occurs at 50% replacement, exhibiting a maximum compressive strength of 126 MPa (+13.5%), a bending strength of 11.6 MPa (+20.8%), and a tensile strength of 7.2 MPa (+6.5%). Moreover, for the same steel slag replacement, 5.1% decrease in the CO_2 eq. emissions was found. However, exceeding the 50% threshold led to a deterioration of UHPC's mechanical properties, and the SEM images revealed that this was mainly caused by the weakened bond between the cement matrix and the aggregates. Thus, it was concluded that the use of steel slag may significantly improve the structural integrity of UHPC when the adequate replacement percentage is adopted (around 50%), being a viable alternative to traditional aggregates that also has environmental advantages (e.g., reduced carbon emissions).

Keywords: mechanical characteristics; carbon footprint; ultra-high-performance concrete (UHPC); silica sand replacement; steel slag

Citation: Bahmani, H.; Mostafaei, H.; Santos, P.; Fallah Chamasemani, N. Enhancing the Mechanical Properties of Ultra-High-Performance Concrete (UHPC) Through Silica Sand Replacement with Steel Slag. *Buildings* **2024**, *14*, 3520. https://doi.org/10.3390/buildings14113520

Academic Editor: Yun Gao

Received: 8 October 2024
Revised: 30 October 2024
Accepted: 31 October 2024
Published: 4 November 2024

1. Introduction

The demand for high-performance construction materials has grown significantly due to the need for structures that can withstand extreme conditions while maintaining durability and efficiency [1–4]. Ultra-High-Performance Concrete (UHPC) has emerged as a revolutionary material in the construction industry, known for its superior mechanical properties, longevity, and versatility [3,5–10]. UHPC's development was driven by the need for concrete that not only meets but exceeds the performance criteria of conventional concrete [11–13].

UHPC distinguishes itself with an exceptional compressive strength, high tensile strength, and enhanced durability, making it suitable for a wide range of applications, from infrastructure to architectural elements [14–16]. Its unique composition, typically characterized by a high cement content, fine aggregates, and fibers, allows for the creation of thinner, lighter structural elements without compromising strength or durability. Despite these advantages, UHPC production faces challenges, particularly related to its cost and the technical complexity of achieving a low water-to-cement ratio [17,18].

In recent years, there has been growing concern over the environmental impact of UHPC, despite its superior mechanical properties and durability. UHPC's high cement content is a significant contributor to its environmental footprint, particularly in terms of greenhouse gas emissions [19,20]. Cement production is responsible for approximately 7–8% of global CO_2 emissions, largely due to the energy-intensive processes involved in the production of clinker, which is a key component of cement. The extensive use of cement in UHPC mixes leads to a high carbon footprint, challenging the sustainability of its applications in the construction industry. As UHPC becomes increasingly used in large-scale infrastructure projects, the need to reduce its environmental impact has become a pressing concern [21–24].

Reducing the carbon footprint of UHPC requires innovative strategies, particularly through the substitution of conventional materials with more sustainable alternatives. A primary area of focus is the replacement of cement or aggregates with industrial by-products, such as steel slag, fly ash, or silica fume, which are often available as waste materials. These materials not only reduce the environmental burden by diverting waste from landfills but also contribute to the mechanical performance of UHPC through pozzolanic reactions and the densification of the microstructure. The incorporation of waste materials into UHPC formulations addresses the dual challenge of enhancing performance while decreasing the material's carbon footprint, aligning with global sustainability goals [10].

Moreover, the cost of steel slag is generally lower than that of silica sand due to its status as an industrial by-product. Thus, utilizing steel slag as a replacement for silica sand can result in significant material cost savings, especially in regions where steel production is abundant.

Several studies have examined the carbon footprint of UHPC and proposed methods to reduce it through material substitutions and mixed design optimizations [25–28]. By optimizing the cement matrix, they enhance UHPC's mechanical properties, resulting in a denser microstructure. This approach not only improves performance but also contributes to sustainability goals [3,14,29–31]. For instance, Randl et al. [32] explored the development of UHPC mixtures from an ecological standpoint, identifying that the inclusion of recycled aggregates and supplementary cementitious materials could significantly reduce the carbon emissions associated with UHPC production. Similarly, Amran et al. [25] analyzed the environmental and mechanical performance of UHPC-containing recycled materials, highlighting the potential for reducing carbon emissions by up to 30% when industrial by-products are utilized. Liu et al. [33] assessed the carbon footprint of UHPC with varying levels of steel slag and found that the environmental impact could be reduced while maintaining or improving the compressive strength of the concrete. These studies underscore the importance of material innovation in reducing the environmental footprint of UHPC, paving the way for more sustainable applications in the construction industry.

A promising approach involves replacing traditional components of UHPC with industrial by-products like steel slag [34–37]. Steel slag, a by-product of steel manufacturing, is rich in reactive and inert components that can influence the properties of concrete. Its incorporation into UHPC as a partial replacement for silica sand offers a dual benefit: it not only utilizes a waste material but also has the potential to enhance the mechanical properties of the concrete through pozzolanic reactions and improved microstructure [38–44].

The integration of steel slag into UHPC formulations has garnered considerable attention in recent research, aiming to enhance mechanical properties and sustainability. Liu and Gou [33] examined the use of steel slag powder and aggregate in UHPC by assessing compressive strength. They indicated that with a cement replacement ratio of up to 10%, the pore structure of pastes with steel slag was comparable to control samples, and UHPC with steel slag powder achieves satisfactory compressive strengths. UHPC incorporating steel slag aggregate displays even higher compressive strengths. Zhang et al. [45] investigated the utilization of steel slag in UHPC, addressing challenges posed by its variable chemical composition and low inherent cementitious properties. The study analyzed its impact on hydration behavior, microstructure, mechanical properties, and volume characteristics of

UHPC mixes. The partial replacement of cement with steel slag initially delayed early-age hydration, resulting in reduced early compressive strength. However, the long-term compressive strength was minimally affected, consistent with a largely unchanged pore structure and compact matrix microstructure observed in backscattered images. Steel slag incorporation did not alter the development pattern of autogenous shrinkage but slightly reduced the autogenous shrinkage strain at higher content levels. Eco-friendliness was demonstrated through leaching toxicity tests and life cycle analyses, highlighting the potential for extended steel slag utilization in eco-friendly UHPC formulations.

Li et al. [46] explored the impact of carbonated fine steel slag as a supplementary cementitious material on UHPC containing coarse aggregates. Their findings indicate that substituting cement with carbonated fine steel slag up to 15% increases C-S-H content, enhancing hydration. Li et al. [47] investigated the application of converter steel slag aggregates (SSA) in UHPC for multifunctional purposes. By optimizing the particle distribution of SSA up to 5.6 mm using a modified packing model, they achieved a high 28-day compressive strength of up to 177.8 MPa and low binder content as low as 567.2 kg/m^3. Fan et al. [48] examined the use of steel slag powder in UHSC. They found that steel slag powder improves workability and wet packing density but reduces early compressive strength due to inhibited cement hydration. Steam curing mitigates these issues, enhancing strength and reducing porosity. Kang et al. [49] evaluated the mechanical properties and self-sensing capabilities of UHPC incorporating steel slag aggregates. Their research revealed that while the compressive and tensile strengths of UHPC with steel slag are slightly lower than those with natural aggregates, steel slag significantly enhances flowability and reduces CO_2 emissions by ~40 kg/m^3. In addressing the environmental challenges associated with steel slag, Mohammad Nejhad et al. [50] investigated its use in UHPC by integrating it with silica fume and zeolite in binary and ternary pozzolan formulations. They evaluated the influence of steel slag and zeolite on UHPC's mechanical and durability properties under various curing conditions. The findings revealed that binary pozzolan mixtures generally outperformed ternary ones. Specifically, incorporating 10% steel slag improved the compressive and flexural strengths by approximately 3.94% and 2.98%, respectively.

Steel slag contains unhydrated lime (CaO), which can cause volumetric instability (expansion). This issue needs to be addressed through proper aging, testing, and quality control of steel slag to ensure its safe application in construction [51,52]. Several studies have focused on stabilizing steel slag to pass the steam test, which includes methods like natural weathering [53], accelerated aging [54], and treatment before cooling [55] or mixing with inert materials [56]. The instability of non-water-quenched slag is linked to the presence of free lime and magnesium oxide [57], as these compounds do not hydrate at normal temperatures during curing [58], leading to long-term expansion and rupture. To prevent such expansion, the free lime content must be reduced to 2–3%; otherwise, the slag is unsuitable for use [59].

While prior studies have explored the impact of replacing silica sand with steel slag, this research uniquely investigates the effects of varying percentages of steel slag on the mechanical properties of UHPC. By systematically examining compressive strength, bending strength, tensile strength, density, and water absorption, this study aims to identify the most effective replacement percentage that maximizes these properties. The insights gained will illuminate how steel slag can be effectively integrated into UHPC formulations, thereby advancing the development of more sustainable, high-performance construction materials. Incorporating steel slag not only addresses the environmental challenges tied to traditional cement production but also fulfills the demand for durable and high-performing concrete solutions. This research contributes a fresh perspective to the field and underscores the potential of steel slag as a valuable resource in cementitious applications.

2. Materials

In the experimental research, ordinary Portland cement was used as the primary binder due to its high quality and consistent chemical composition, as shown in Table 1. Steel slag, a by-product of steel manufacturing, was incorporated with a particle size of less than 150 microns, making it suitable for inclusion in the UHPC mix. The fine particle size of the steel slag facilitated effective integration and bonding within the concrete. Silica fume (or micro-silica), recognized for its super pozzolanic properties, was utilized to enhance the strength and durability of the concrete. This silica fume, produced in electric arc furnaces and resembling grey powdered Portland cement or fly ash, adheres to ASTM C1240 standards [60] and was obtained from the Iran Ferroalloy Company, with a density of 2200 kg/m^3. Silica sand was sourced from the Chirok mine sand factory, with particles smaller than 150 microns. Table 1 lists the chemical compositions of the materials used. The specific weight of the steel slag used was approximately 2800 kg/m^3, while the silica sand had a specific weight of around 2600 kg/m^3. Additionally, the granularity of the aggregates was consistent with findings from previous research [5–7]. These density values are crucial for understanding the results discussed later in the study, particularly in relation to the overall density of the cement mortar/UHPC. The denser steel slag contributed to the increase in density observed in UHPC samples as the slag replacement percentage increased. The impact of these densities on the final UHPC mix will be further analyzed in the results section.

Table 1. Chemical compositions of the used materials (% by weight).

	Cement	Silica Fume	Steel Slag
Aluminum oxide (Al_2O_3)	5.5	0.6	5.4
Silicon dioxide (SiO_2)	21.9	95	17.08
Iron oxide (Fe_2O_3)	3.4	0.3	25.45
Calcium oxide (CaO)	61	1.5	29.93
Magnesium oxide (MgO)	2.3	1	10.58
Sulphur trioxide (SO_3)	2.3	---	---
Mn_2O_3	---	---	8.91
K_2O	0.6	---	0.13
Na_2O	0.3	---	0.12
Loss on ignition (LOI)	2.7	1.6	2.4
Moisture content	---	0.01–0.4	---

The particle size distribution of both silica sand and steel slag used in this study is shown in Figure 1. The distribution demonstrates that both materials fall within a similar size range, with most particles between 100 and 300 µm. Steel slag particles exhibit a slightly coarser distribution compared to silica sand, which can influence the packing density and microstructure of the UHPC. The denser packing of steel slag is beneficial for improving the mechanical properties.

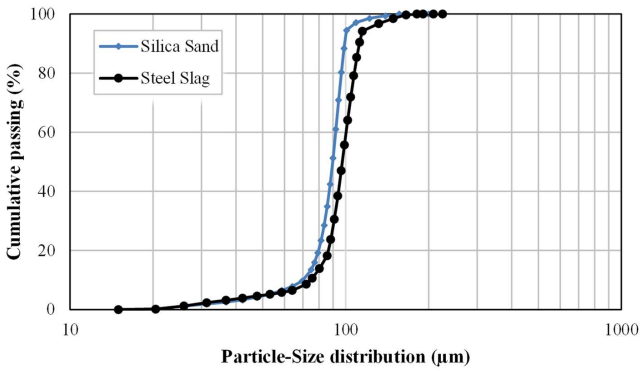

Figure 1. Particle size distribution of both silica sand and steel slag used in this study.

To maintain a consistent water-to-cement ratio and achieve homogeneity, superplasticizer (SP) materials were employed. AURAMIX 4450 (FOSROC, Dubai, UAE), based on polycarboxylate ether and compliant with ASTM C494 standards [61], was used to enhance concrete fluidity [62]. Efforts were made to achieve a target slump of approximately 170 mm for the samples. The distinct mix designs are provided in Table 2, with symbols such as 'UHPC' for the reference mix, and '25%SS', '50%SS', '75%SS', and '100%SS' for mixtures replacing silica sand with steel slag (SS) at varying percentages.

Table 2. Mixture proportions in the present research.

Designation	Cement (kg/m^3)	Silica Fume (kg/m^3)	Silica Sand (kg/m^3)	Steel Slag (kg/m^3)	W/B [1]	SP [2] (kg/m^3)
UHPC (Ref.)	950	285	863	–	0.17	24.7
UHPC (25%SS)	950	285	647	216	0.17	26.7
UHPC (50%SS)	950	285	431.5	431.5	0.17	28.7
UHPC (75%SS)	950	285	216	647	0.17	30.7
UHPC (100%SS)	950	285	–	863	0.17	32.7

[1] W/B—Water–Binder ratio; [2] SP—Superplasticizer.

For each mix design, three samples were prepared and tested for compressive strength, tensile strength, and flexural strength to ensure the accuracy and reliability of the results. This approach allowed for consistent measurement and comparison of the mechanical properties of the UHPC mixtures with varying percentages of steel slag replacement. The average values from these three tests were used to assess the overall performance of each mix.

The test specimens underwent standard curing in water for 28 days. Figure 2 shows the samples before they were tested. Cylindrical samples measuring 100 mm in diameter and 200 mm in height were used for the compressive strength tests (ASTM C496 [63]), as illustrated in Figure 2a. Prismatic test specimens measuring 70 × 70 × 350 mm (ASTM C78 [64]) were used for the flexural tests, as displayed in Figure 2b.

(**a**) (**b**)

Figure 2. Specimens before being tested: (**a**) cylindrical (100 × 200 mm) for compressive strength tests; (**b**) prismatic (70 × 70 × 350 mm) for flexural strength tests.

3. Test Setup and Methods

This section presents the experimental procedures and methodologies employed in evaluating the performance of UHPC with different percentages of steel slag substitution for silica sand. The tests conducted include water absorption, density measurements, compressive strength, tensile strength, flexural strength, and Scanning Electron Microscopy (SEM) analysis. These tests provide comprehensive insights into the mechanical properties, microstructural characteristics, and environmental performance of UHPC. Additionally, the

carbon footprint of the different concrete mixtures was analyzed to assess the sustainability benefits of using steel slag as a replacement material.

3.1. Water Absorption and Density

To determine the water absorption percentage of the specimens, the procedure followed the guidelines of ASTM C642 (Standard Test Method for Density, Absorption, and Voids in Hardened Concrete). The specimens were immersed in water at room temperature for a period of 24 h. The water absorption percentage was calculated by comparing the mass of the specimens before and after immersion. Specifically, the dry weight of the samples was recorded after oven-drying them at 100 to 110 °C for a minimum of 24 h. After immersion, the specimens were surface-dried and re-weighed to obtain the saturated weight. The water absorption percentage was determined by the equation

$$Water\ Absorption\ (\%) = \frac{Saturated\ Weight - Dry\ Weight}{Dry\ Weight} \times 100 \quad (1)$$

This method ensures an accurate measurement of the material's porosity and permeability, providing valuable insights into the durability and impermeability of the concrete samples.

For the density measurements, the samples were also tested following the ASTM C642 standard [65]. The density was determined by measuring the dry mass and the volume of the specimens. The volume was calculated by measuring the dimensions of the specimens or by the water displacement method, depending on the sample size and geometry. This method was chosen to ensure an accurate assessment of the concrete's mass-to-volume ratio.

3.2. Mechanical Resistance

In this study, the compressive strength of UHPC was assessed using a 2000 kN hydraulic jack, as depicted in Figure 3a, in accordance with the ASTM C39 [66] standard guidelines. This evaluation is crucial because compressive strength directly affects other properties such as tensile strength, elasticity, and water absorption, making it essential for understanding the overall performance of UHPC. For tensile strength assessment, the Brazilian test method was employed, following ASTM C496 [63] specifications, using the cylindrical samples previously illustrated in Figure 2a. Furthermore, the four-point flexural test was conducted to evaluate the bending strength of the concrete. This test followed the ASTM C78 [64] standards and included specific details related to sample size, device setup, and testing procedure. Prismatic specimens, previously showed in Figure 2b, were tested in this flexural test, using a testing machine capable of applying up to 50 kN of force, as shown in Figure 3b.

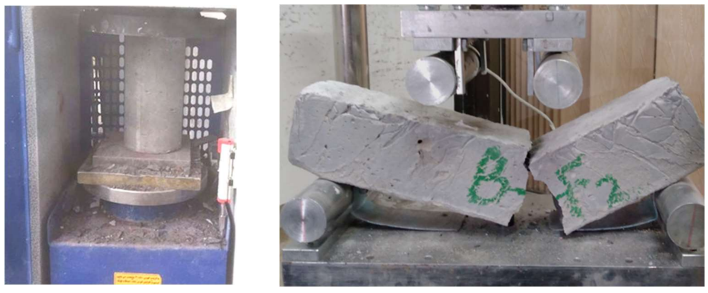

(**a**) (**b**)

Figure 3. Test setup: (**a**) compressive strength; (**b**) flexural strength.

3.3. SEM Analysis

For the SEM analysis, the methodology adhered to the relevant practices outlined in ASTM C1723 [67]. The SEM analysis was conducted to examine the microstructure and

interfacial properties between the cement matrix and the aggregates, especially focusing on the influence of steel slag incorporation at various percentages using HITACHI S-4160 SEM (Tokyo, Japan) at 36 kV.

Small fragments of the concrete samples were carefully extracted and coated with a thin layer of gold to enhance conductivity. The samples were then placed in the SEM chamber, and a high-energy electron beam was used to scan the surface at varying magnifications. The SEM analysis provided detailed images of the microstructural changes, revealing the morphology of the hydration products, the porosity, and the bonding quality between the cementitious matrix and the aggregates.

3.4. Carbon Footprint Emissions

For the carbon footprint analysis in this study, SimaPro version 9.6 software was employed, utilizing the IMPACT 2002+ methodology to assess the environmental impacts associated with the production of UHPC. SimaPro is a robust and widely used life cycle assessment (LCA) tool that allows for detailed environmental analysis by modeling the entire lifecycle of a product or material. It incorporates various databases and methodologies to evaluate the emissions and resource consumption.

The carbon footprint assessment followed a cradle-to-gate approach, considering the extraction and processing of raw materials, transportation, and production processes. This approach provides a comprehensive view of the environmental impacts up until the product's manufacturing stage. The IMPACT 2002+ method integrates several midpoint and endpoint categories, focusing on key environmental impacts such as global warming potential, which is critical for determining the carbon footprint.

Data for the analysis were drawn from reliable databases embedded within SimaPro, which include region-specific emission factors and production data for materials such as steel slag, silica sand, and Portland cement. The software's modeling capabilities allowed for the calculation of CO_2 emissions associated with various percentages of steel slag substitution in UHPC. The accuracy of this assessment was ensured by adopting internationally recognized standards such as ISO 14040 [68] and ISO 14044 [69], which outline the framework for conducting LCAs.

By using SimaPro and the IMPACT 2002+ method, the analysis not only quantified the carbon emissions but also highlighted the environmental benefits of incorporating steel slag, a recycled material, into the UHPC mix. The reduction in emissions due to the replacement of virgin materials with steel slag demonstrates the potential for lowering the overall carbon footprint in construction materials.

4. Results and Discussion

In this section, the results of the water absorption, density, compressive strength, tensile strength, flexural strength tests, SEM analysis, and carbon footprint emissions are presented and discussed in detail.

4.1. Water Absorption

Figure 4 presents the water absorption percentages for samples incorporating various proportions of steel slag. The reference mixing design for UHPC demonstrates the lowest water absorption percentage at 2.1%, reflecting UHPC's inherent properties of dense microstructure and low water-to-cementitious materials ratio, which contribute to its exceptional impermeability. As the proportion of steel slag increased—from partial substitution to complete replacement—there was a corresponding rise in water absorption. This trend can be attributed to the nature of steel slag, a by-product of steel manufacturing, which introduces both reactive and inert components into the mix. The integration of steel slag affects the concrete's overall porosity and permeability, with higher slag content leading to the formation of additional pores and capillaries. This results in increased water absorption. The maximum water absorption percentage, observed in the mix design with 100% steel slag, reached 4.8%, which is a 2.7% increase. These findings underscore the significant

impact of steel slag content on the water absorption characteristics of UHPC, highlighting the need to balance slag incorporation to optimize impermeability and durability.

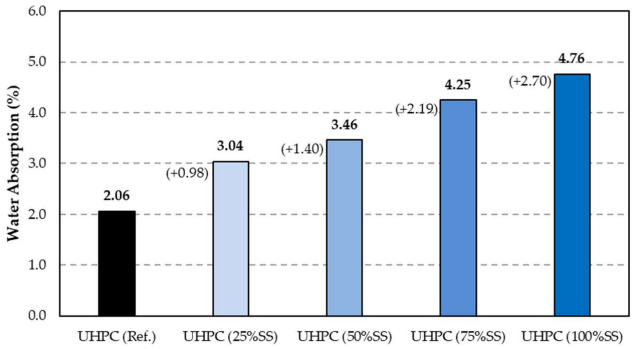

Figure 4. Water absorption results for UHPC samples.

The observed increase in water absorption with higher steel slag content can be attributed to several factors related to the microstructure and particle characteristics of the steel slag itself. While steel slag does exhibit pozzolanic activity, which typically improves the microstructure of concrete by reacting with calcium hydroxide to form additional cementitious materials, the overall impact on porosity is influenced by the particle size distribution and intrinsic characteristics of the slag.

Firstly, steel slag particles tend to have a coarser distribution compared to the finer silica sand. This difference in particle size affects the packing density within the concrete matrix, leading to the formation of additional voids and capillaries, which in turn increase water absorption. Despite the potential pozzolanic reaction, the presence of these voids limits the ability of the concrete to form a denser, impermeable structure.

Secondly, steel slag may have a relatively high intrinsic porosity and higher water absorption capacity compared to silica sand. This characteristic contributes to the increased water absorption observed at higher replacement levels. The steel slag particles themselves can absorb more water, introducing additional free water into the mix that may not fully participate in the hydration process, leaving behind capillaries and increasing overall porosity.

This effect counters the expected pozzolanic benefit, as the pozzolanic reaction would typically reduce porosity by densifying the microstructure. However, the dominance of the particle size distribution and intrinsic porosity of steel slag overrides this effect, leading to increased absorption. The balance between these competing effects—particle size, porosity, and pozzolanic reaction—is crucial for understanding the performance of steel slag in UHPC formulations.

4.2. Density

Figure 5 illustrates the density of samples with varying percentages of steel slag substitution for silica sand. The data reveal a clear trend: as the percentage of steel slag increases, so does the density of the concrete samples. Steel slag, due to its higher density compared to silica sand, adds more mass to the concrete. Consequently, higher steel slag content results in an increased density. The base mixing design exhibits the lowest density at 2386 kg/m^3, which is expected given the absence of steel slag's denser contribution. The mix containing 100% steel slag achieved the highest density of 2894 kg/m^3, which reflects the significant influence of steel slag's higher specific gravity compared to silica sand. The increase in density by 21.3% can be explained by the denser nature of steel slag particles, which replace the lighter silica sand, thus contributing to the overall mass of the concrete. This progression highlights the significant influence of steel slag on the density of the concrete, emphasizing its role in enhancing the overall density of the material. These findings align with the inherent properties of steel slag and underscore its impact on the mass and density characteristics of UHPC.

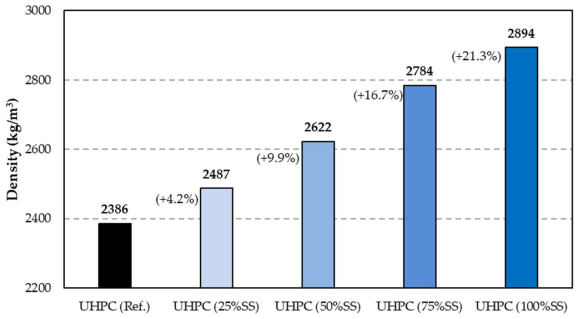

Figure 5. Density results for UHPC samples.

4.3. Compressive Strength

Figure 6 illustrates the compressive strength results for concrete mixtures with varying percentages of steel slag replacing silica sand. Analysis of the data reveals a notable trend: as the replacement percentage of silica sand by steel slag increases to 50%, the compressive strength of the mixtures improves by 13%. This enhancement is attributed to the pozzolanic properties of steel slag, which reacts with calcium hydroxide to form additional binding materials, thereby boosting the overall strength of the concrete. The highest compressive strength recorded is 126 MPa, achieved in the mixture containing 50% steel slag, demonstrating the optimal balance between steel slag reactivity and the cementitious matrix. Beyond this 50% replacement threshold, a diminishing trend is observed, with compressive strength decreasing by 26 MPa (from 126 MPa to 100 MPa) as the replacement percentage increases from 50% to 100%. This reduction in strength is likely due to the excessive steel slag content, which can negatively impact the hydration process and disrupt the matrix structure. Therefore, the findings suggest that a 50% replacement of silica sand with steel slag provides the optimal balance for enhancing compressive strength in these concrete mixtures. One explanation is the pozzolanic reactivity of steel slag, which enhances the formation of additional calcium silicate hydrate (C-S-H), strengthening the matrix. However, it is important to consider other mechanisms, such as particle packing efficiency and the intrinsic porosity of the slag.

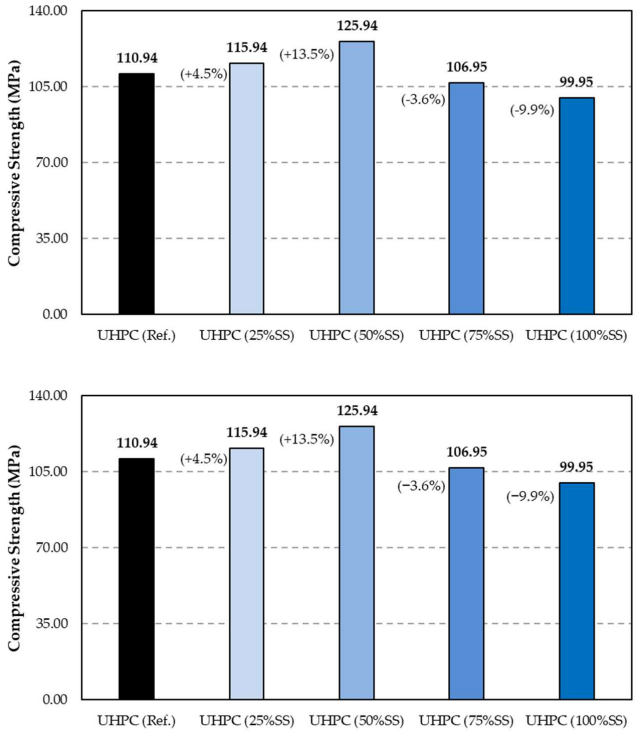

Figure 6. Compressive strength results for UHPC samples.

4.4. Tensile Strength

Figure 7 illustrates the tensile strength results for UHPC samples incorporating varying percentages of steel slag as a replacement for silica sand. The results reveal that the tensile strength of the mixtures increases as the replacement percentage of silica sand with steel slag rises up to 50%, achieving a notable improvement of 7%. The enhancement in strength observed with the inclusion of steel slag can be attributed to its pozzolanic properties, which contribute to the concrete's overall strength and improve the bonding within the matrix. Steel slag contains reactive oxides, such as silica (SiO_2) and alumina (Al_2O_3), that react with calcium hydroxide (produced during cement hydration) to form additional calcium silicate hydrate (C-S-H), densifying the matrix. The peak tensile strength of 7.2 MPa is observed in the mixture with 50% steel slag, underscoring the beneficial impact of steel slag at this substitution level. However, when the replacement percentage exceeds 50%, the tensile strength begins to decline. Specifically, the tensile strength decreases from 7.2 MPa to 4.96 MPa as the replacement percentage of steel slag increases from 50% to 100%. This reduction, amounting to 2.2 MPa, may be due to the excessive steel slag content, which could disrupt the matrix balance and weaken interparticle bonds. Consequently, the optimal replacement percentage of silica sand with steel slag is determined to be 50%, beyond which the tensile strength benefits diminish, aligning with trends observed in compressive strength results.

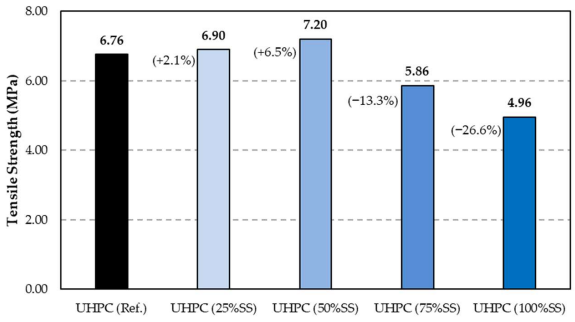

Figure 7. Tensile strength results for UHPC samples.

4.5. Flexural Strength

The flexural strength results for concrete mixtures incorporating varying percentages of steel slag as a replacement for silica sand are presented in Figure 8. The findings show that the flexural strength of the mixtures improves as the proportion of silica sand replaced by steel slag increases up to 50%, with a notable enhancement of 2 MPa. This improvement aligns with the anticipated benefits of steel slag, which enhances concrete strength due to its pozzolanic properties. The pozzolanic reaction between steel slag and calcium hydroxide generates additional binding material, thereby increasing the overall flexural strength. The highest flexural strength of 11.6 MPa is observed in the mixture containing 50% steel slag, indicating the optimal synergy between the slag and the cementitious matrix at this replacement level. However, as the steel slag content exceeds 50%, the flexural strength begins to decline. Specifically, a decrease of 3 MPa is noted when the replacement percentage increases from 50% to 100%. The strength enhancement observed with 50% steel slag (SS) replacement at 28 days can be attributed to an optimal balance between the pozzolanic activity of the steel slag and its physical properties. At this replacement level, the steel slag reacts with calcium hydroxide to form additional C-S-H, which improves the bonding and densifies the concrete matrix. This results in increased compressive and tensile strength due to improved microstructural cohesion. However, beyond 50% replacement, the coarser particle size and intrinsic porosity of steel slag become detrimental, disrupting particle packing and increasing void content, which weakens the matrix and leads to a decrease in strength. Thus, while 50% SS optimally enhances strength, higher slag content negatively affects performance due to poor packing and higher porosity, particularly at later stages of curing.

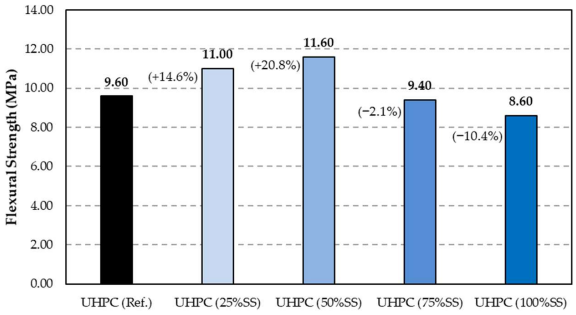

Figure 8. Flexural strength results for UHPC samples.

4.6. SEM Analysis

The scanning electron microscopy (SEM) analysis was conducted on samples containing varying percentages of steel slag—specifically 50%, 75%, and 100%—to explore the underlying reasons for the observed decline in mechanical properties as the percentage of steel slag increased from 50% to 100%. This investigation aimed to provide a comprehensive understanding of how the incorporation of steel slag affects the structural integrity and performance of the material. In the images presented in Figure 9, the hydration products, specifically calcium silicate hydrate (C-S-H) and calcium hydroxide (CH), are clearly identifiable. The distinct morphology and distribution of these compounds can be observed, highlighting the formation and interaction of these key hydration products within the cement matrix.

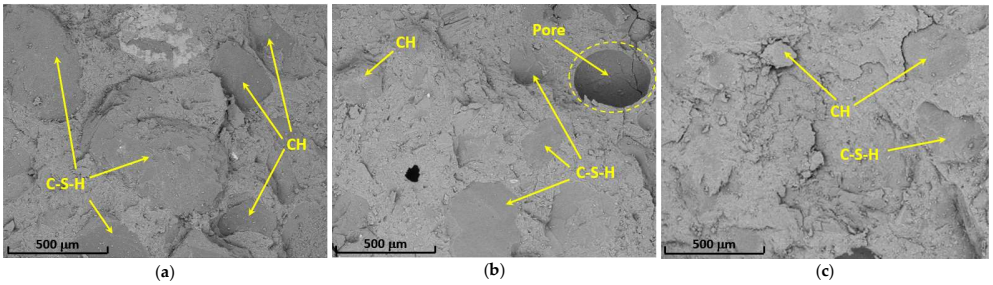

Figure 9. SEM images: (**a**) UHPC (50%SS); (**b**) UHPC (75%SS); (**c**) UHPC (100%SS).

In UHPC, the cement, silica fume, and water undergo a hydration that forms C-S-H. The C-S-H gel fills the voids between the fine aggregates (like silica sand), creating a dense and compact matrix. This dense matrix can obscure the visibility of individual sand particles in SEM images, as the sand particles are well embedded in the surrounding cementitious paste. Moreover, the silica sand used in UHPC is typically very fine, often less than 600 microns. These fine particles blend seamlessly into the cement matrix, especially after hydration, making it difficult to distinguish them from the surrounding material in SEM images. Furthermore, UHPC contains silica fume, which reacts with CH produced during cement hydration to form additional C-S-H.

As illustrated in Figure 9, the SEM analysis revealed that the bond between the cement matrix and the aggregate becomes increasingly compromised with the higher steel slag content. This weakening of the cement–aggregate interface is a key factor contributing to the deterioration in mechanical characteristics. The SEM images clearly depict the morphological changes occurring at the microstructural level, highlighting the reduced interfacial adhesion that occurs as more steel slag is introduced into the mixture.

Furthermore, the analysis also showed an increase in the formation of calcium hydroxide (CH) hydration products within the cement paste as the steel slag content was raised. The accumulation of these CH crystals can disrupt the overall microstructure and cohesion of the cement matrix, leading to a reduction in the mechanical performance of the material. The presence of excessive CH can create a less stable microenvironment, which

may hinder the effective bonding of particles and compromise the overall strength of the composite material.

Consequently, these findings from the SEM analysis suggest that the deterioration in mechanical characteristics is directly linked to the rising percentage of steel slag in the mixture. The weakening of the cement–aggregate bond and the increased presence of CH hydration products appear to be the primary mechanisms responsible for the observed decline in mechanical properties as the steel slag content is increased from 50% to 100%. This analysis underscores the importance of carefully considering the proportion of steel slag used in concrete formulations to maintain optimal mechanical performance and structural integrity.

4.7. Carbon Footprint Emission

Figure 10 presents the carbon footprint results for concrete mixtures incorporating different percentages of steel slag as a replacement for silica sand. The results reveal a significant environmental benefit from incorporating steel slag as a recycled material. With the application of a negative emission factor for steel slag, the carbon footprint progressively decreases as the percentage of steel slag increases. At 100% replacement, the carbon footprint drops from 893.5 kg CO_2eq/m^3 in the reference mix to 802.9 kg CO_2eq/m^3, representing a substantial reduction. This decrease highlights the environmental savings associated with the reuse of industrial waste, which not only reduces emissions but also mitigates the need for virgin materials. Furthermore, the combination of enhanced mechanical properties and reduced carbon emissions makes steel slag an ideal sustainable alternative for silica sand in UHPC, contributing to both structural performance and sustainability goals. The synergy between mechanical improvement and environmental savings underscores the viability of steel slag in eco-friendly concrete formulations, aligning with global efforts to minimize the carbon footprint in the construction industry.

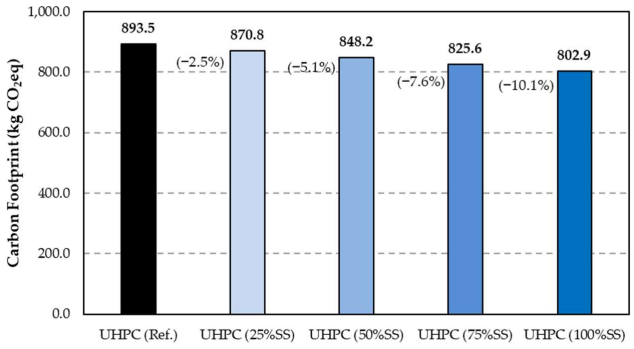

Figure 10. Carbon footprint results for UHPC samples.

This study has made significant progress in exploring the mechanical properties and sustainability of UHPC with steel slag as a partial replacement for silica sand. However, certain limitations must be acknowledged. First, this research focused primarily on short-term mechanical properties, while long-term performance, including durability and resilience over extended periods, was not within the scope of the study. Furthermore, this study did not fully address the volume stability of UHPC incorporating steel slag, particularly the potential expansion issues related to unhydrated lime and magnesium oxide present in steel slag. These aspects are crucial for practical applications and should be considered in future research.

Future studies should build upon these findings by investigating higher replacement levels of steel slag to fully understand its potential in enhancing UHPC performance. Long-term durability studies under various environmental conditions will provide valuable insights into the practical viability of UHPC with steel slag in real-world construction projects. Additionally, an in-depth investigation into the volume stability of concrete containing steel slag is necessary, particularly focusing on mitigating potential expansion

caused by free lime and magnesium oxide. Understanding how to stabilize these components is critical for ensuring the material's longevity and structural integrity. Further exploration of optimizing mix designs through the inclusion of various additives and supplementary cementitious materials is also essential to maximize both the mechanical properties and sustainability of UHPC. By addressing these research directions, future studies can contribute to the development of more sustainable and high-performance concrete, advancing global efforts to reduce the construction industry's carbon footprint.

5. Conclusions

In this research work, the mechanical properties of UHPC were enhanced by replacing silica sand with steel slag at several percentages (25% up to 100% with 25% increment). These improvements were measured and quantified by performing several standardized lab tests. Moreover, the carbon emissions were also computed.

The following main conclusions were found:

- The base mixing design (UHPC) exhibited the lowest water absorption percentage at 2.1%, which aligns with its dense microstructure and low water-to-cementitious materials ratio. Conversely, the highest water absorption was recorded in the mixture with 100% steel slag (+4.8%), indicating increased porosity.
- The lowest relative density of 2386 kg/m^3 was observed in the reference UHPC mix, reflecting the impact of silica sand on density. In contrast, the highest density of 2894 kg/m^3 (+21.3%) was achieved in the mix containing 100% steel slag, which underscores the substantial contribution of steel slag to the overall mass and density of this UHPC.
- The replacement of silica sand with steel slag up to 50% resulted in optimal mechanical properties. Specifically, a compressive strength of 126 MPa (a 13.5% increase), a bending strength of 11.6 MPa (a 20.8% increase), and a tensile strength of 7.2 MPa (a 6.5% increase) were observed at this replacement level. However, exceeding the 50% replacement threshold led to a noticeable decline in these mechanical performance values.
- The SEM images revealed that the mechanical performance decrease, observed as the percentage of steel slag increased from 50% to 100%, was primarily due to the weakening bond between the cement matrix and the aggregates. This reduced bond is attributed to the smaller adhesion and interaction at the aggregates' interface, which compromises the overall structural integrity of this composite material.
- The use of steel slag led to a noticeable decrease in carbon emissions, particularly at higher substitution levels. The reduction in carbon footprint by approximately 10% at full replacement (100% steel slag) highlights the potential of steel slag to contribute to increased sustainable construction practices.

Despite the significant strides made in this research, certain limitations are acknowledged. Firstly, the study was limited to investigating the effects of steel slag replacement of silica sand for only four percentages: 25%, 50%, 75% and 100%. This restriction means that the impact of intermediate replacement levels remains unexplored. Additionally, the research focused on the short-term mechanical properties of UHPC. Long-term performance, including durability and resilience over time, was not within the scope of this study. Another limitation is the lack of a comprehensive environmental impact assessment, besides the evaluated carbon footprint related to using steel slag as a silica sand replacement in UHPC. Moreover, as future work, it would be interesting to modify the mix ratio in Table 2 and adopt the equal volume method, instead of the equal mass method.

Author Contributions: Conceptualization, H.M., H.B. and P.S.; methodology, H.M., H.B. and P.S.; formal analysis, H.M., H.B., P.S. and N.F.C.; investigation, H.M., H.B. and N.F.C.; resources, H.M. and H.B.; data curation, H.M., H.B. and N.F.C.; writing—original draft preparation, H.M., H.B. and N.F.C.; writing—review and editing, H.M., H.B. and P.S.; visualization, H.M., H.B., P.S. and N.F.C.; supervision, H.M., H.B. and P.S. All authors have read and agreed to the published version of the manuscript.

Funding: This research received no external funding.

Data Availability Statement: The data presented in this study are available on request from the corresponding author. The data are not publicly available due to confidentiality issues.

Conflicts of Interest: The authors declare no conflicts of interest.

References

1. Aıtcin, P.C. The durability characteristics of high performance concrete: A review. *Cem. Concr. Compos.* **2003**, *25*, 409–420. [CrossRef]
2. Li, V.C. Large volume, high-performance applications of fibers in civil engineering. *J. Appl. Polym. Sci.* **2002**, *83*, 660–686. [CrossRef]
3. Du, J.; Meng, W.; Khayat, K.H.; Bao, Y.; Guo, P.; Lyu, Z.; Abu-Obeidah, A.; Nassif, H.; Wang, H. New development of ultra-high-performance concrete (UHPC). *Compos. Part B Eng.* **2021**, *224*, 109220. [CrossRef]
4. Neville, A.; Aitcin, P.-C. High performance concrete—An overview. *Mater. Struct.* **1998**, *31*, 111–117. [CrossRef]
5. Bahmani, H.; Mostofinejad, D. Comparative analysis of environmental, social, and mechanical aspects of high-performance concrete with calcium oxide-activated slag reinforced with basalt, and recycled PET fibers. *Case Stud. Constr. Mater.* **2024**, *20*, e02895. [CrossRef]
6. Bahmani, H.; Mostofinejad, D.; Dadvar, S.A. Mechanical properties of ultra-high-performance fiber-reinforced concrete containing synthetic and mineral fibers. *ACI Mater. J.* **2020**, *117*, 155–168.
7. Bahmani, H.; Mostofinejad, D.; Dadvar, S.A. Fiber type and curing environment effects on the mechanical performance of UHPFRC containing zeolite. *Iran. J. Sci. Technol. Trans. Civ. Eng.* **2022**, *46*, 4151–4167. [CrossRef]
8. Habel, K.; Viviani, M.; Denarié, E.; Brühwiler, E. Development of the mechanical properties of an ultra-high performance fiber reinforced concrete (UHPFRC). *Cem. Concr. Res.* **2006**, *36*, 1362–1370. [CrossRef]
9. Kim, D.J.; Park, S.H.; Ryu, G.S.; Koh, K.T. Comparative flexural behavior of hybrid ultra high performance fiber reinforced concrete with different macro fibers. *Constr. Build. Mater.* **2011**, *25*, 4144–4155. [CrossRef]
10. Mostafaei, H.; Bahmani, H.; Mostofinejad, D.; Wu, C. A novel development of HPC without cement: Mechanical properties and sustainability evaluation. *J. Build. Eng.* **2023**, *76*, 107262. [CrossRef]
11. Bahmani, H.; Mostafaei, H.; Ghiassi, B.; Mostofinejad, D.; Wu, C. *A Comparative Study of Calcium Hydroxide, Calcium Oxide, Calcined Dolomite, and Metasilicate as Activators for Slag-Based HPC*; Elsevier: Amsterdam, The Netherlands, 2023; p. 105653.
12. Bahmani, H.; Mostofinejad, D. Strength development and microstructure properties of slag activated with alkaline earth metal ions: A review study. *Eur. J. Environ. Civ. Eng.* **2023**, *27*, 4497–4527. [CrossRef]
13. Bahmani, H.; Mostofinejad, D. High-performance concrete based on alkaline earth metal ions-activated slag at ambient temperature: Mechanical and microstructure properties. *J. Mater. Res. Technol.* **2023**, *24*, 8703–8724. [CrossRef]
14. Amran, M.; Huang, S.-S.; Onaizi, A.M.; Makul, N.; Abdelgader, H.S.; Ozbakkaloglu, T. Recent trends in ultra-high performance concrete (UHPC): Current status, challenges, and future prospects. *Constr. Build. Mater.* **2022**, *352*, 129029. [CrossRef]
15. Zhou, M.; Lu, W.; Song, J.; Lee, G.C. Application of ultra-high performance concrete in bridge engineering. *Constr. Build. Mater.* **2018**, *186*, 1256–1267. [CrossRef]
16. Yu, Z.; Wu, L.; Yuan, Z.; Zhang, C.; Bangi, T. *Retracted: Mechanical Properties, Durability and Application of Ultra-High-Performance Concrete Containing Coarse Aggregate (UHPC-CA): A Review*; Elsevier: Amsterdam, The Netherlands, 2022; Volume 334.
17. Abdal, S.; Mansour, W.; Agwa, I.; Nasr, M.; Abadel, A.; Onuralp Özkılıç, Y.; Akeed, M.H. Application of ultra-high-performance concrete in bridge engineering: Current status, limitations, challenges, and future prospects. *Buildings* **2023**, *13*, 185. [CrossRef]
18. Sharma, R.; Jang, J.G.; Bansal, P.P. A comprehensive review on effects of mineral admixtures and fibers on engineering properties of ultra-high-performance concrete. *J. Build. Eng.* **2022**, *45*, 103314. [CrossRef]
19. Mostafaei, H.; Kelishadi, M.; Bahmani, H.; Wu, C.; Ghiassi, B. Development of sustainable HPC using rubber powder and waste wire: Carbon footprint analysis, mechanical and microstructural properties. *Eur. J. Environ. Civ. Eng.* **2024**, 1–22. [CrossRef]
20. Aghamohammadi, O.; Mostofinejad, D.; Mostafaei, H.; Abtahi, S.M. Mechanical properties and impact resistance of concrete pavement containing crumb rubber. *Int. J. Geomech.* **2024**, *24*, 04023242. [CrossRef]
21. Mostafaei, H.; Keshavarz, Z.; Rostampour, M.A.; Mostofinejad, D.; Wu, C. Sustainability evaluation of a concrete gravity dam: Life cycle assessment, carbon footprint analysis, and life cycle costing. *Structures* **2023**, *53*, 279–295. [CrossRef]
22. Mostafaei, H.; Badarloo, B.; Chamasemani, N.F.; Rostampour, M.A.; Lehner, P. Investigating the effects of concrete mix design on the environmental impacts of reinforced concrete structures. *Buildings* **2023**, *13*, 1313. [CrossRef]
23. Chamasemani, N.F.; Kelishadi, M.; Mostafaei, H.; Najvani, M.A.D.; Mashayekhi, M. Environmental Impacts of Reinforced Concrete Buildings: Comparing Common and Sustainable Materials: A Case Study. *Constr. Mater.* **2023**, *4*, 1–15. [CrossRef]
24. Tayari, S.; Abedi, R.; Tahvildari, K. Experimental investigation on fuel properties and engine characteristics of biodiesel produced from *Eruca sativa*. *SN Appli. Sci.* **2020**, *2*, 2. [CrossRef]
25. Amran, M.; Murali, G.; Makul, N.; Tang, W.C.; Alluqmani, A.E. Sustainable development of eco-friendly ultra-high performance concrete (UHPC): Cost, carbon emission, and structural ductility. *Constr. Build. Mater.* **2023**, *398*, 132477. [CrossRef]

26. Qian, D.; Yu, R.; Shui, Z.; Sun, Y.; Jiang, C.; Zhou, F.; Ding, M.; Tong, X.; He, Y. A novel development of green ultra-high performance concrete (UHPC) based on appropriate application of recycled cementitious material. *J. Clean. Prod.* **2020**, *261*, 121231. [CrossRef]
27. Bajaber, M.A.; Hakeem, I.Y. UHPC evolution, development, and utilization in construction: A review. *J. Mater. Res. Technol.* **2021**, *10*, 1058–1074. [CrossRef]
28. Imam, A.; Sharma, K.K.; Kumar, V.; Singh, N. A review study on sustainable development of ultra high-performance concrete. *AIMS Mater. Sci.* **2022**, *9*, 9–35. [CrossRef]
29. Kathirvel, P.; Sreekumaran, S. Sustainable development of ultra high performance concrete using geopolymer technology. *J. Build. Eng.* **2021**, *39*, 102267. [CrossRef]
30. Shao, R.; Wu, C.; Li, J.; Liu, Z. Development of sustainable steel fibre-reinforced dry ultra-high performance concrete (DUHPC). *J. Clean. Prod.* **2022**, *337*, 130507. [CrossRef]
31. Wang, J.N.; Yu, R.; Ji, D.D.; Tang, L.W.; Yang, S.C.; Fan, D.Q.; Shui, Z.H.; Leng, Y.; Liu, K.N. Effect of distribution modulus (q) on the properties and microstructure development of a sustainable Ultra-High Performance Concrete (UHPC). *Cem. Concr. Compos.* **2022**, *125*, 104335. [CrossRef]
32. Randl, N.; Steiner, T.; Ofner, S.; Baumgartner, E.; Mészöly, T. Development of UHPC mixtures from an ecological point of view. *Constr. Build. Mater.* **2014**, *67*, 373–378. [CrossRef]
33. Liu, J.; Guo, R. Applications of Steel Slag Powder and Steel Slag Aggregate in Ultra-High Performance Concrete. *Adv. Civ. Eng.* **2018**, *2018*, 1426037. [CrossRef]
34. Sun, G.; Du, M.; Shan, B.; Shi, J.; Qu, Y. Ultra-high performance concrete design method based on machine learning model and steel slag powder. *Case Stud. Constr. Mater.* **2022**, *17*, e01682. [CrossRef]
35. Tang, X.; He, B.; Yang, B.; Chen, J. Experimental Study on Axial Stress–Strain Behaviour of Steel Fibre-Reinforced Steel Slag Micropowder UHPC. *Appl. Sci.* **2023**, *13*, 8807. [CrossRef]
36. Sun, G.; Shi, J.; Qu, Y. Cracking and yield behavior of reinforced UHPC beams containing steel slag under flexural test. *Eng. Struct.* **2023**, *280*, 115693. [CrossRef]
37. Tang, X.; Feng, C.; Chang, J.; Ma, J.; Hu, X. Research on the flexural performance of steel pipe steel slag powder ultra-high-performance concrete components. *Materials* **2023**, *16*, 5960. [CrossRef]
38. Li, S.; Cheng, S.; Mo, L.; Deng, M. Effects of steel slag powder and expansive agent on the properties of ultra-high performance concrete (UHPC): Based on a case study. *Materials* **2020**, *13*, 683. [CrossRef] [PubMed]
39. Peng, Y.Z.; Chen, K.; Hu, S.G. Durability and microstructure of ultra-high performance concrete having high volume of steel slag powder and ultra-fine fly ash. *Adv. Mater. Res.* **2011**, *255*, 452–456. [CrossRef]
40. Shi, K.; Deng, H.; Hu, J.; Zhou, J.; Cai, X.; Liu, Z. Effects of steel slag powder content and curing condition on the performance of alkali-activated materials based UHPC matrix. *Materials* **2023**, *16*, 3875. [CrossRef]
41. Liu, G.; Schollbach, K.; Li, P.; Brouwers, H.J.H. Valorization of converter steel slag into eco-friendly ultra-high performance concrete by ambient CO_2 pre-treatment. *Constr. Build. Mater.* **2021**, *280*, 122580. [CrossRef]
42. Mu, X.; Zhang, S.; Ni, W.; Xu, D.; Li, J.; Du, H.; Wei, X.; Li, Y. Performance optimization and hydration mechanism of a clinker-free ultra-high performance concrete with solid waste based binder and steel slag aggregate. *J. Build. Eng.* **2023**, *63*, 105479. [CrossRef]
43. Fan, D.; Yu, R.; Shui, Z.; Liu, K.; Feng, Y.; Wang, S.; Li, K.; Tan, J.; He, Y. A new development of eco-friendly Ultra-High performance concrete (UHPC): Towards efficient steel slag application and multi-objective optimization. *Constr. Build. Mater.* **2021**, *306*, 124913. [CrossRef]
44. Xu, J.; Zhan, P.; Zhou, W.; Zuo, J.; Shah, S.P.; He, Z. Design and assessment of eco-friendly ultra-high performance concrete with steel slag powder and recycled glass powder. *Powder Technol.* **2023**, *419*, 118356. [CrossRef]
45. Zhang, X.; Zhao, S.; Liu, Z.; Wang, F. Utilization of steel slag in ultra-high performance concrete with enhanced eco-friendliness. *Constr. Build. Mater.* **2019**, *214*, 28–36. [CrossRef]
46. Li, S.; Liu, G.; Yu, Q. The role of carbonated steel slag on mechanical performance of ultra-high performance concrete containing coarse aggregates. *Constr. Build. Mater.* **2021**, *307*, 124903. [CrossRef]
47. Li, P.; Jiang, J.; Liu, G.; Ren, Z. Physical, mechanical, thermal and sustainable properties of UHPC with converter steel slag aggregates. *Case Stud. Constr. Mater.* **2022**, *17*, e01458. [CrossRef]
48. Fan, D.; Zhang, C.; Lu, J.-X.; Liu, K.; Yin, T.; Dong, E.; Yu, R. Recycling of steel slag powder in green ultra-high strength concrete (UHSC) mortar at various curing conditions. *J. Build. Eng.* **2023**, *70*, 106361. [CrossRef]
49. Kang, M.; Kang, M.-C.; Yonis, A.; Vashistha, P.; Pyo, S. Effect of steel slag on the mechanical properties and self-sensing capability of ultra-high performance concrete (UHPC). *Dev. Built Environ.* **2024**, *17*, 100342. [CrossRef]
50. Mohammad Nezhad Ayandeh, M.H.; Ghodousian, O.; Mohammad Nezhad, H.; Mohtasham Moein, M.; Saradar, A.; Karakouzian, M. Steel slag and zeolite as sustainable pozzolans for UHPC: An experimental study of binary and ternary pozzolan mixtures under various curing conditions. *Innov. Infrastruct. Solut.* **2024**, *9*, 265. [CrossRef]
51. Wang, G.; Wang, Y.; Gao, Z. Use of steel slag as a granular material: Volume expansion prediction and usability criteria. *J. Hazard. Mater.* **2010**, *184*, 555–560. [CrossRef]
52. Ameri, M.; Behnood, A. Laboratory studies to investigate the properties of CIR mixes containing steel slag as a substitute for virgin aggregates. *Constr. Build. Mater.* **2012**, *26*, 475–480. [CrossRef]

53. Saffari, R.; Habibagahi, G.; Nikooee, E.; Niazi, A. Biological stabilization of a swelling fine-grained soil: The role of microstructural changes in the shear behavior. *J. Sci. Technol. Trans. Civ. Eng.* **2017**, *41*, 405–414. [CrossRef]
54. da Silveira, N.O.; e Silva, M.V.A.M.; Agrizzi, E.J.; de Lana, M.F.; da Silva, E.A.; de Mendonça, R.L. ACERITA®-Steel slag with reduced expansion potential. *Metall. Res. Technol.* **2004**, *101*, 779–785. [CrossRef]
55. Sorrentino, F.; Gimenez, M.; Crumbie, A. Mineralogy of modified steel slags. In Proceedings of the 11th International Congress on the Chemistry of Cement (ICCC), Durban, South Africa, 11–16 May 2003; pp. 2139–2147.
56. Deneele, D.; De Larrard, F.; Rayssac, E.; Reynard, J. Control of basic oxygen steel slag swelling by mixing with inert material. In Proceedings of the 4th European Slag Conference (Euroslag), Oulu, Finland, 20–21 June 2005; pp. 20–21.
57. Geiseler, J. Use of steelworks slag in Europe. *Waste Manag.* **1996**, *16*, 59–63. [CrossRef]
58. Chengmu, L.I.; Wanjun, L.I. Discussion on quality & expansiveness of expansive material-magnesium oxide. *Des. Hydroelectr. Power Stn.* **2005**, *3*, 95–99.
59. Kuo, W.-T.; Shu, C.-Y. Application of high-temperature rapid catalytic technology to forecast the volumetric stability behavior of containing steel slag mixtures. *Constr. Build. Mater.* **2014**, *50*, 463–470. [CrossRef]
60. *ASTM C1240*; Standard Specification for Silica Fume Used in Cementitious Mixtures. ASTM International: Philadelphia, PA, USA, 2017.
61. *ASTM C494*; Standard Specification for Chemical Admixtures for Concrete. ASTM International: West Conshohocken, PA, USA, 2015.
62. Dadvar, S.A.; Mostofinejad, D.; Bahmani, H. Strengthening of RC columns by ultra-high performance fiber reinforced concrete (UHPFRC) jacketing. *Constr. Build. Mater.* **2020**, *235*, 117485. [CrossRef]
63. *ASTM C496*; Standard Test Method for Splitting Tensile Strength of Cylindrical Concrete Specimens. ASTM C496/C496M; ASTM: West Conshohocken, PA, USA, 2017.
64. *ASTM C78-09*; Standard Test Method for Flexural Strength of Concrete (Using Simple Beam with Third-Point Loading). American Society for Testing and Materials: West Conshohocken, PA, USA, 2010.
65. *ASTM C642-21*; Standard Test Method for Density, Absorption, and Voids in Hardened Concrete. ASTM International: West Conshohocken, PA, USA, 2021.
66. *ASTM C39/C39M17*; Standard Test Method for Compressive Strength of Cylindrical Concrete Specimens. ASTM International: West Conshohocken, PA, USA, 2017.
67. *ASTM C1723-16*; Standard Guide for Examination of Hardened Concrete Using Scanning Electron Microscopy. American Society of Testing and Materials: West Conshohocken, PA, USA, 2010; Volume 4, p. 2.
68. *ISO 14040*; Environmental Management-Life Cycle Assessment—Principles and Framework. ISO—International Organization for Standardization: Geneva, Switzerland, 2006.
69. *ISO 14044*; Environmental Management-Life Cycle Assessment—Requirements and Guidelines. ISO—International Organization for Standardization: Geneva, Switzerland, 2006.